Hyperfine Interactions (2021) 242: 16
https://doi.org/10.1007/s10751-021-01732-8

Comparison of the ^{57}Fe hyperfine parameters for iron-bearing phases in some undifferentiated and differentiated meteorites

M. I. Oshtrakh[1] · A.A. Maksimova[1,2]

Accepted: 26 September 2021/ Published online: 29 October 2021

Abstract
A comparison of the ^{57}Fe hyperfine parameters obtained for the iron-bearing phases in some undifferentiated and differentiated meteorites using Mössbauer spectroscopy demonstrate some similarities and small differences for the same phases in different meteorites. These differences were related to small variations in the iron local microenvironments in these phases that may be a result of some variations in the chemical compositions and thermal metamorphism. The latter variations can be associated with these phases' formation and thermal evolution in space.

Keywords ^{57}Fe hyperfine parameters · Mössbauer spectroscopy · Undifferentiated and differentiated meteorites · iron-bearing phases

1 Introduction

Meteorites are significant space messengers which carry an important information about formation and evolution of the Solar System. All meteorites chemically divided into three groups (stony, stony-iron and iron meteorites) can be considered as undifferentiated and differentiated within the modern classification [1]. Undifferentiated meteorites are the most

This article is part of the Topical Collection on *Proceedings of the International Conference on Hyperfine Interactions (HYPERFINE 2021), 5-10 September 2021, Brasov, Romania*
Edited by Ovidiu Crisan

✉ M. I. Oshtrakh
oshtrakh@gmail.com

A.A. Maksimova
alia55@bk.ru

1 Institute of Physics and Technology, Ural Federal University, Ekaterinburg, Russian Federation 620002

2 The Zavaritsky Institute of Geology and Geochemistry of the Ural Branch of the Russian Academy of Sciences, Ekaterinburg, Russian Federation 620110

primitive meteorites which were formed with the Solar System while differentiated meteorites are the result of thermal metamorphism of the matter in asteroids and protoplanets (parent bodies) with further differentiation. All meteorites contain various iron-bearing phases such as olivine (Fe, Mg)$_2$SiO$_4$, orthopyroxene (Fe, Mg)SiO$_3$, Ca-poor and Ca-rich clinopyroxene (Fe, Ca, Mg)SiO$_3$, Fe-Ni-Co alloy, troilite FeS, chromite FeCr$_2$O$_4$, hercynite FeAl$_2$O$_4$, ilmenite FeTiO$_3$ and some other phases [2, 3]. Therefore, meteorites are the subject of the studies by Mössbauer spectroscopy about 60 years (see for review [4, 5] and references therein). Taking into account various extreme factors affecting meteorites or matter in their parent bodies (thermal metamorphism, shock and reheating, very slow cooling, etc.) in space, it is interesting to compare the ^{57}Fe hyperfine parameters for the same phases in different meteorites which were measured using Mössbauer spectroscopy with a high velocity resolution, i.e., with a higher discretization of the velocity reference signal (2^{12}) that increases precision, sensitivity and accuracy of Mössbauer spectroscopy.

2 Experimental

Undifferentiated meteorites represent various ordinary chondrites: Ochansk H4, Richardton H5, Vengerovo H5, Annama H5, Zvonkov H6, Saratov L4, Kemer L4, Farmington L5, Mbale L5/6, Mount Tazerzait L5, Tsarev L5–1 (fragment No 1), Tsarev L5–2 (fragment No 2), Kunashak L6, Ozerki L6, Bursa L6, Bjurböle L/LL4, five fragments of Chelyabinsk LL5 with different lithologies numbered No 1, No 1a, No 2, No 2a and No 3, Northwest Africa (NWA) 6286 LL6 and NWA 7857 LL6. Differentiated meteorites represent Seymchan main group pallasite (PMG), which is a stony-iron meteorite, and Sariçiçek howardite, which is a stony achondrite originated from asteroid (4) Vesta [6]. Preparation and characterization of these meteorites by optical and scanning electron microscopy (SEM) with energy dispersive spectroscopy (EDS), X-ray diffraction (XRD), Mössbauer spectroscopy and some other techniques were described in detail elsewhere [7–17].

The room temperature Mössbauer spectra of meteorite samples were measured using an automated precision Mössbauer spectrometric system, built on the base of the SM-2201 spectrometer, with a saw-tooth shape velocity reference signal formed by the digital-analog converter using discretization of 2^{12} (quantification of the velocity reference signal using 4096 steps). Details and characteristics of this spectrometer and the system as well as this method's features were described in [18, 19]. The (1.8–1.0) × 10^9 Bq ^{57}Co in rhodium matrix sources (Ritverc GmbH, St. Petersburg) were used at room temperature. The Mössbauer spectra were measured in transmission geometry with moving absorber and recorded in 4096 channels. Then these spectra were converted into 1024-channel spectra by consequent summation of four neighboring channels to increase the signal-to-noise ratio for the minor spectral components.

Mössbauer spectra were computer fitted using UNIVEM-MS program by the least squares procedure with a Lorentzian line shape. The troilite magnetic sextet in the Mössbauer spectra of meteorites was fitted using simulation of the full static Hamiltonian described in detail in [20]. Moreover, these spectra were decomposed taken into account components related to ^{57}Fe in the M1 and M2 sites in silicate crystals (olivine, orthopyroxene and clinopyroxene) as well as to the minor phases of chromite, hercynite, ilmenite and paramagnetic γ-Fe(Ni, Co) phase, etc. (see [21]). The spectral parameters such as isomer shift, δ, quadrupole splitting (taken to be equal to 2ε, where ε is the quadrupole shift for magnetically split spectra), ΔE_Q, magnetic hyperfine field, H_{eff}, line width, Γ, relative subspectrum (component) area, A, and statistical quality of the fit, χ^2, were determined. We were unable to determine 2ε for troilite in the case of simulation of the full static Hamiltonian. The thin reference absorbers of α-Fe foil with a thickness of 7 μm and sodium nitroprusside with a thickness of 5 mg Fe/cm^2 were used for the large and small velocity scale calibration, respectively, and for the control of the velocity driving system (the line shapes of the spectra were pure Lorentzian). An instrumental (systematic) error for each spectrum point was ±0.5 channel (the velocity scale), the instrumental (systematic) error for the hyperfine parameters was ±1 channel in mm/s or kOe. If an error calculated with the fitting procedure (fitting error) for these parameters exceeded the instrumental (systematic) error, the larger error was used instead. Criteria of the best fit were differential spectrum, the value of χ^2, and physical meaning of parameters. Values of δ are given relative to α-Fe at 295 K.

3 Results and discussion

Examples of the measured room temperature Mössbauer spectra of selected undifferentiated and differentiated meteorites with their best fits are shown in Fig. 1. The main and minor spectral components were assigned to the following iron-bearing phases on the basis of the ^{57}Fe hyperfine parameters: the ferromagnetic α_2-Fe(Ni, Co), α-Fe(Ni, Co) and γ-Fe(Ni, Co) phases, the paramagnetic γ-Fe(Ni, Co) phase, troilite and pyrrhotite $Fe_{1-x}S$ (we can consider this as near stoichiometric or nonstoichiometric troilite if $0 < x \leq 0.05$ [22]), olivine (M1 and M2 sites), orthopyroxene (M1 and M2 sites), Ca-poor and Ca-rich clinopyroxene (M1 and M2 sites), chromite, hercynite, magnesiochromite $Mg_{1-x}Fe_xCr_2O_4$, ilmenite, some unknown ferrous and ferric compounds and ferrihydrite $5Fe_2O_3 \times 9H_2O$ in the case of terrestrial weathering. These phases were confirmed by SEM with EDS and XRD. It should be noticed that Seymchan PMG contains no orthopyroxene while Sariçiçek howardite contains no olivine.

A comparison of the ^{57}Fe hyperfine parameters obtained for spectral components associated with the M1 and M2 sites in olivine, orthopyroxene and clinopyroxene are shown on the plots of ΔE_Q vs. δ in Fig. 2. These plots demonstrate some scattering of parameters for each site in each silicate phase. It is possible to observe some regions of parameters where silicate phases in different meteorites are similar within the errors as well as differences between some regions beyond the errors. These variations may reflect small differences in the ^{57}Fe local microenvironments in the M1 and M2 sites in olivine, orthopyroxene and clinopyroxene. At least two reasons of these differences can be considered such as (i) variations of the total Fe^{2+} and Mg^{2+} contents in these silicate phases and (ii) differences of the Fe^{2+} and Mg^{2+} cations distribution among the M1 and M2 sites in each silicate phase.

It is well known that the unit cell parameters (*a*, *b* and *c*) of olivine crystals depend on the total Fe^{2+} relative content X_{Fe}. This was demonstrated in [23] using the ICDD database PDF2. Basing on these linear relations and the unit cell parameters obtained from XRD, we determined X_{Fe} for olivine in the studied meteorites (an example of this relation for *a* and X_{Fe} for olivine is demonstrated in Fig. 3). An increase of the X_{Fe} values for olivine (or fayalite Fa, a molar fraction of Fe_2SiO_4 in olivine) in ordinary chondrites from group H to group LL is well known [24]. Olivine in Sariçiçek howardite contains the lowest X_{Fe} value. Thus, one of the reasons of the iron local microenvironment variations is related to small

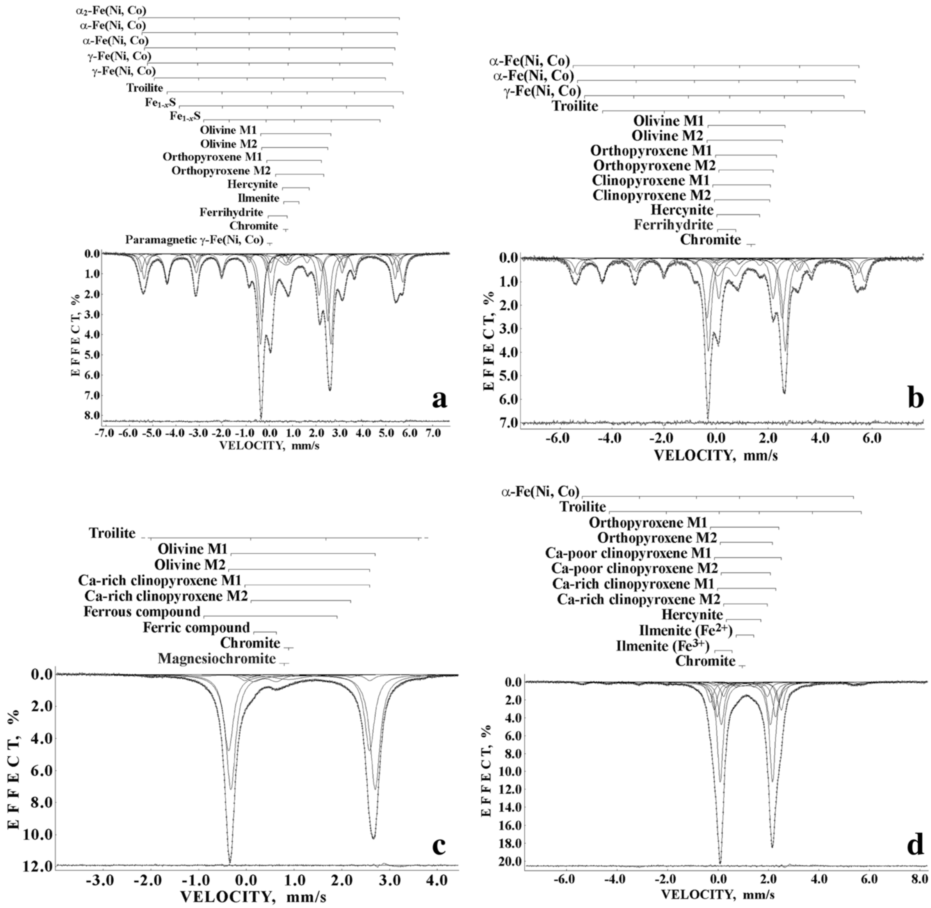

Fig. 1 Mössbauer spectra of undifferentiated meteorites: ordinary chondrites Bursa L6 (***a***) and Kemer L4 (***b***), and differentiated meteorites: stony part of Seymchan main group pallasite (*c*) and Sariçiçek howardite (*d*). Indicated components are the results of the best fits. The differential spectra are shown on the bottom. T = 295 K

differences of the unit cell parameters in olivine and other silicate crystals with variations of the X_{Fe} values.

Variations in the Fe^{2+} and Mg^{2+} cations distribution among the M1 and M2 sites in silicate crystals can also affect the iron local microenvironment. Therefore, small variations of ΔE_Q and δ values in Fig. 2 reflect tiny differences in the iron local microenvironments in olivine, orthopyroxene and clinopyroxene in the studied undifferentiated and differentiated meteorites resulting from various factors including the total iron content and Fe^{2+} and Mg^{2+} partitioning among the M1 and M2 sites in silicate crystals. These variations are related to differences of the silicate phases formation and their thermal history in space.

A comparison of the ^{57}Fe hyperfine parameters deduced for troilite component in the Mössbauer spectra of studied undifferentiated and differentiated meteorites is shown in the plot of H_{eff} vs. δ (Fig. 4). This plot demonstrates some scattering of the H_{eff} values for different meteorites. Earlier it was shown that appearance of the iron vacancies in pyrrhotites leads to a

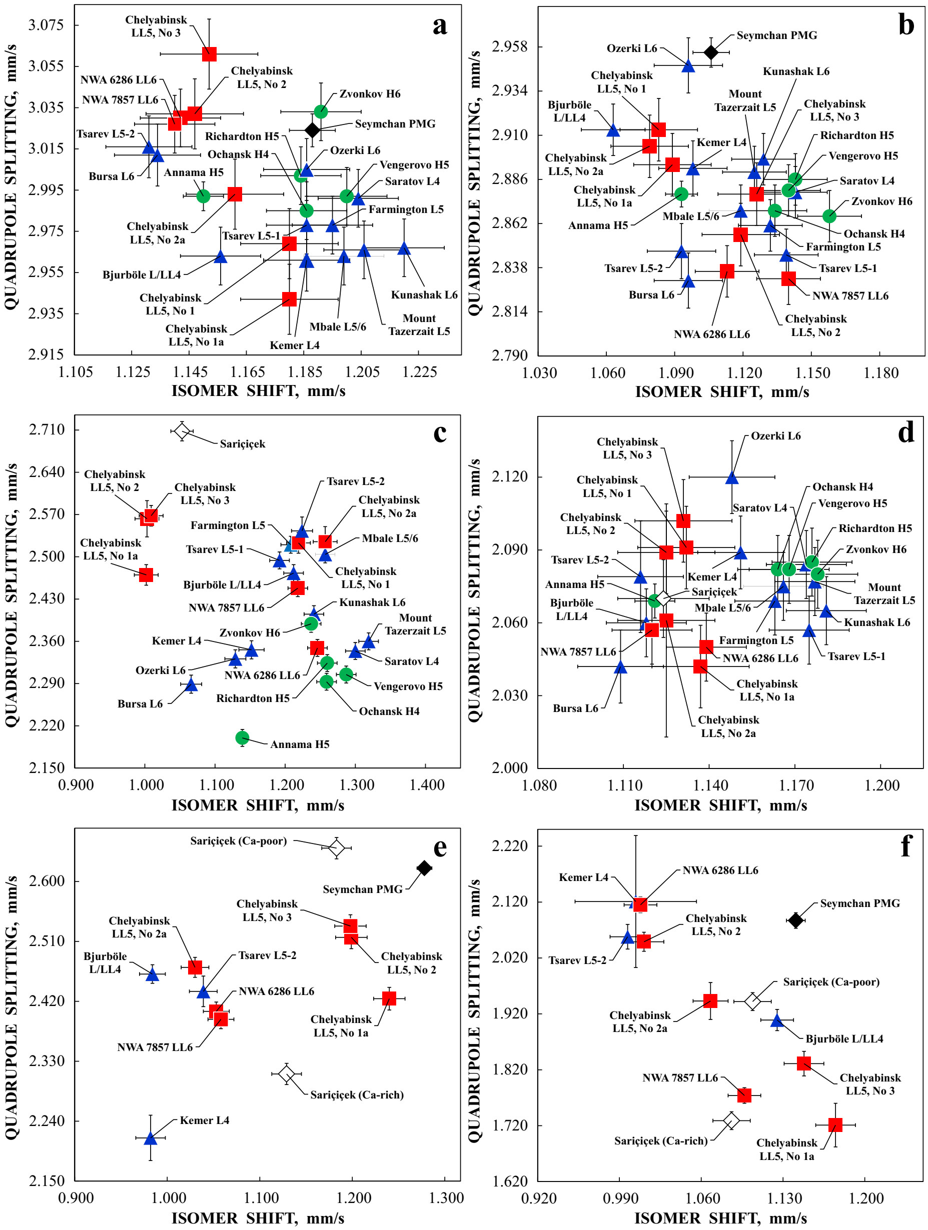

Fig. 2 The ^{57}Fe hyperfine parameters for the M1 and M2 sites in olivine (***a*** and ***b***), orthopyroxene (***c*** and ***d***) and clinopyroxene (***e*** and ***f***) in undifferentiated (●, ▲, ■) and differentiated (◆ and ◇) meteorites. ● – H ordinary chondrites, ▲ – L ordinary chondrites, ■ – LL ordinary chondrites, ◆ – main group pallasite, ◇ – howardite

decrease of the H_{eff} values [25]. This also may be a result of small variations in the iron local microenvironment in troilite from different meteorites because the unit cell parameters for pyrrhotites ($a = b$ and c) are linearly related to the nonstoichiometry parameter x as shown in

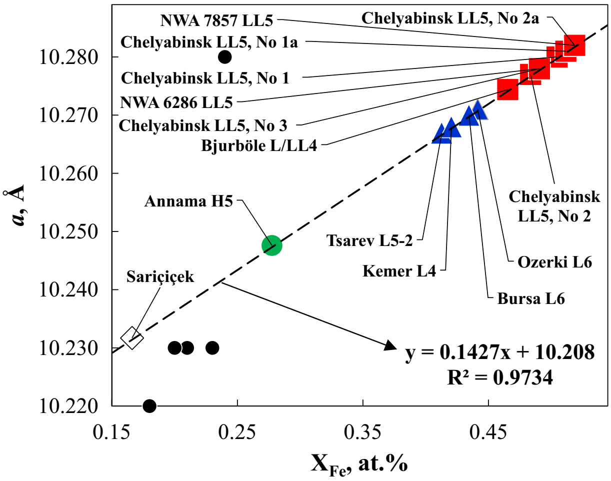

Fig. 3 Determination of the total Fe^{2+} relative content X_{Fe} in olivine crystals from selected meteorites using the unit cell parameter *a* deduced from XRD. ● – data for olivines from ICDD database PDF2 fitted by linear dependence in [23] (a part of data are shown), ● – H ordinary chondrites, ▲ – L ordinary chondrites, ■ – LL ordinary chondrites, ◇ – howardite

Fig. 5 using the data from [25]. The range for the nonstoichiometry parameter was taken $0 \leq x \leq 0.0150$, i.e. for stoichiometric and near stoichiometric troilite. Therefore, small iron deficiency causes small variations in the iron local microenvironment that may be reflected by the ^{57}Fe hyperfine parameters. It should be noticed that increasing of iron deficiency in troilite may be related to the thermal effects. Therefore, the smallest values of H_{eff} in Fig. 4 can be

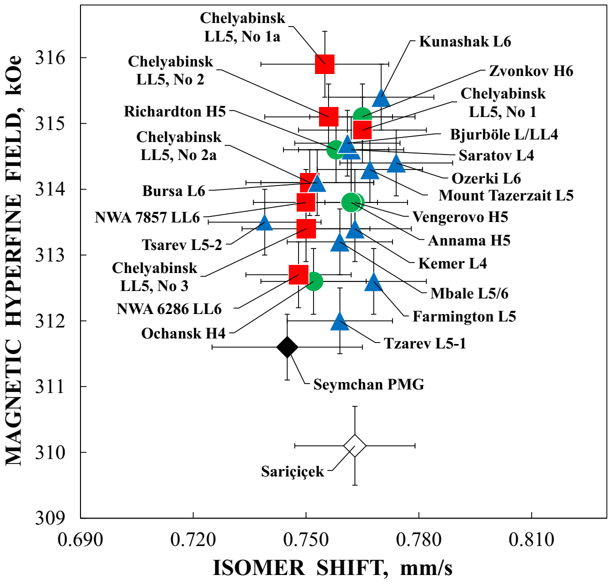

Fig. 4 Comparison of the ^{57}Fe hyperfine parameters for troilite component in the Mössbauer spectra of undifferentiated (●, ▲, ■) and differentiated (◆ and ◇) meteorites. ● – H ordinary chondrites, ▲ – L ordinary chondrites, ■ – LL ordinary chondrites, ◆ – main group pallasite, ◇ – howardite

associated with relatively higher iron vacancies in troilite inclusions resulting from the effect of higher thermal metamorphism.

A comparison of the ^{57}Fe hyperfine parameters for both ferromagnetic α-Fe(Ni, Co) and γ-Fe(Ni, Co) phases in the metal grains in ordinary chondrites and howardite is shown in the plots of H_{eff} vs. δ in Fig. 6. These data also demonstrate some distribution of the ^{57}Fe hyperfine parameters for the α-Fe(Ni, Co) and γ-Fe(Ni, Co) phases. Moreover, it was possible to reveal more than one magnetic sextet assigned to the α-Fe(Ni, Co) phase in the Mössbauer spectra of some ordinary chondrites while two magnetic sextets associated with the γ-Fe(Ni, Co) phase were detected in the Mössbauer spectrum of Annama H5 only. Several magnetic sextets related to one phase were explained as a result of variations of the number of Ni atoms in the iron local microenvironments in the metal grains as shown by SEM with EDS. Earlier results for the b.c.c. α-Fe(Ni) and f.c.c. γ-Fe(Ni) alloys with variations in Ni content demonstrated that the average values of H_{eff} vary in both alloys with Ni content (see [26, 27]). In the case of Seymchan PMG, it was possible to separate metal alloy and stony part of meteorite. Therefore, the Mössbauer spectrum of separated Fe-Ni-Co alloy was measured much better than that in the bulk mixture of various phases in other meteorites. It was possible to decompose this spectrum using two sextets for α_2-Fe(Ni, Co), four sextets for α-Fe(Ni, Co) and two sextets for γ-Fe(Ni, Co) phases. The values of H_{eff} for the corresponding phases were in the same ranges as for other meteorites.

A comparison of the ^{57}Fe hyperfine parameters for hercynite in the studied meteorites is presented in the plot of ΔE_Q vs. δ in Fig. 7. Some small variations in the ^{57}Fe hyperfine parameters can also be seen.

SEM with EDS demonstrated that hercynite can be considered in chromite inclusions due to the presence of Al as the third metal besides Cr and Fe in the latter with a content in the range ~2–3.5 wt%. In fact, hercynite can be considered as $FeAl_2O_4$ and/or mixed spinel $Fe(Al_{1-x}Cr_x)_2O_4$ microcrystals with small x values (XRD revealed the presence of hercynite). Earlier studies of synthetic $FeAl_2O_4$ and that with partial substitutions of Fe by Mg, Mn and some other metals and Al partial substitution by Cr showed variations in the ^{57}Fe hyperfine parameters, e.g., ΔE_Q values varied in the range 1.17–1.57 mm/s [28] (see also, e.g., [29–31]). Taking into consideration the presence of tiny contents of accessory metals such as Mg, Mn and Ti determined by SEM with EDS besides Cr, Fe and Al in chromite inclusions in the studied meteorites except Seymchan PMG, we can suggest some variations in the iron local microenvironments in hercynite and/or mixed spinel $Fe(Al_{1-x}Cr_x)_2O_4$ microcrystals in

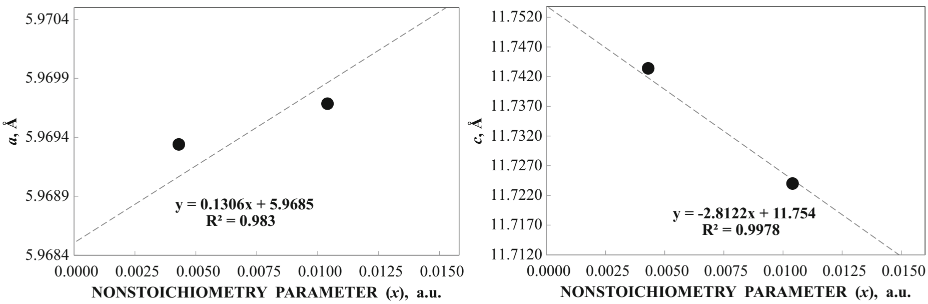

Fig. 5 Fragments of the linear dependencies of the unit cell parameters of pyrrhotites $Fe_{1-x}S$ on the nonstoichiometry parameter x in the range $0 \le x \le 0.0150$ (● − data taken from [25])

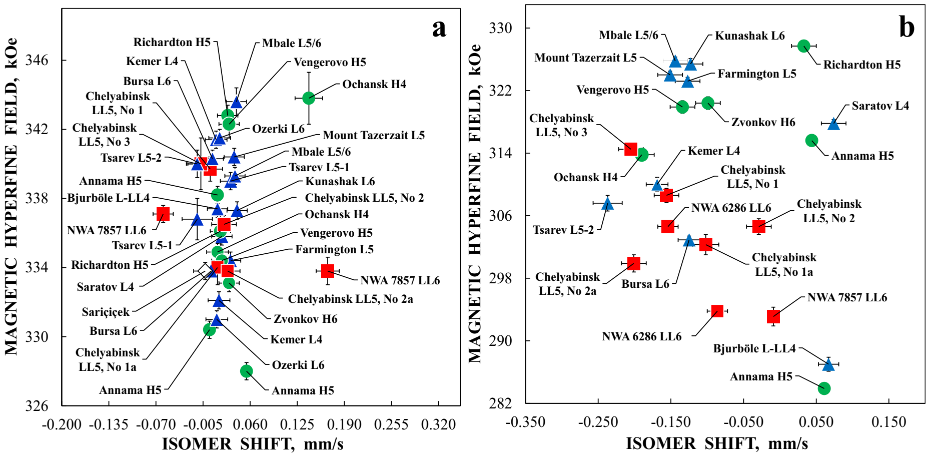

Fig. 6 Comparison of the ^{57}Fe hyperfine parameters for the α-Fe(Ni, Co) phase (***a***) and the ferromagnetic γ-Fe(Ni, Co) phase (***b***) components in the Mössbauer spectra of undifferentiated (●, ▲, ■) and differentiated (◇) meteorites. ● – H ordinary chondrites, ▲ – L ordinary chondrites, ■ – LL ordinary chondrites, ◇ – howardite

chromite that may be reflected by the ^{57}Fe hyperfine parameters. As for Seymchan PMG, chemical analysis by SEM with EDS showed the presence of Mg as the third metal in chromite inclusions instead of Al. Therefore, the presence of magnesiochromite $(Fe_{1-x}Mg_x)Cr_2O_4$ in chromite was supposed instead of hercynite in Seymchan PMG and confirmed by XRD and Mössbauer spectroscopy.

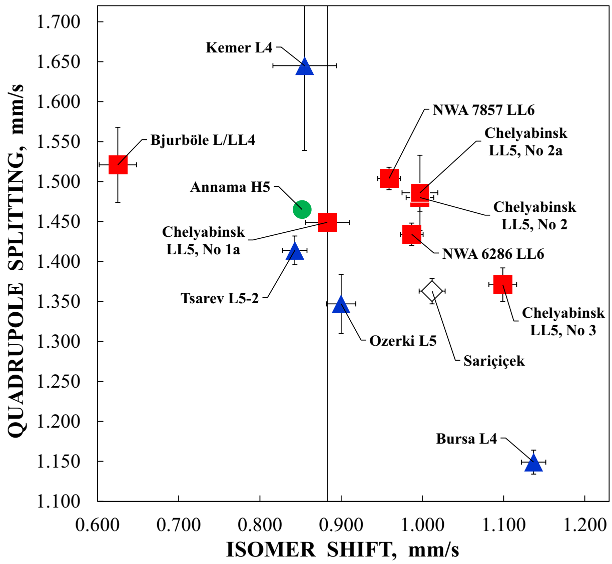

Fig. 7 Comparison of the ^{57}Fe hyperfine parameters for hercynite component in the Mössbauer spectra of undifferentiated (●, ▲, ■) and differentiated (◇) meteorites. ● – H ordinary chondrites, ▲ – L ordinary chondrites, ■ – LL ordinary chondrites, ◇ – howardite

4 Conclusion

Comparison of the ^{57}Fe hyperfine parameters for olivine, orthopyroxene, clinopyroxene, troilite, α-Fe(Ni, Co), γ-Fe(Ni, Co) and hercynite crystals in the studied undifferentiated and differentiated meteorites demonstrates some similarities and some differences for the same phases in different meteorites. The observed differences were associated with the corresponding variations in the iron local microenvironments in these phases. These variations can be related in part to the small concentration differences, the presence of accessory atoms and thermal effects. Small variations in the ^{57}Fe hyperfine parameters and iron local microenvironments in the M1 and M2 sites in silicate phases can be a result of (i) different Fe content and (ii) different distributions of Fe^{2+} and Mg^{2+} cations among the M1 and M2 sites in the same silicate crystals in different meteorites. These variations are associated with different formation processes and thermal history of silicate phases in space in the studied meteorites. Small variations in the ^{57}Fe hyperfine parameters and iron local microenvironments in troilite inclusions can be a result of small iron deficiency formed due to thermal metamorphism in space. Small variations in the ^{57}Fe hyperfine parameters and iron local microenvironments in the α-Fe(Ni, Co) and γ-Fe(Ni, Co) phases in the metal grains may be a result of corresponding Ni and Co concentration variations related to the Fe-Ni-Co alloy formation and further thermal evolution in space. Small variations in the ^{57}Fe hyperfine parameters and iron local microenvironments in hercynite and/or $Fe(Al_{1-x}Cr_x)_2O_4$ microcrystals in chromite inclusions in different meteorites can be a result of the small concentration variations of accessory metals (Mg, Mn, Ti, etc.) that may be associated with chromite formation and evolution in space. Thus, the ^{57}Fe hyperfine parameters with data obtained by other complementary techniques appeared to be useful for the analysis of the iron local microenvironment in the iron-bearing phases and its variations in different meteorites.

Acknowledgements This work was supported by the Ministry of Science and Higher Education of the Russian Federation, project № FEUZ-2020-0060. The Zavaritsky Institute of Geology and Geochemistry of the Ural Branch of the Russian Academy of Sciences is supported by the Ministry of Science and Higher Education of the Russian Federation, project № AAAA-A19-119071090011-6 (A.A.M.).

References

1. Weisberg, M.K., McCoy, T.J., Krot, A.N.: Systematics and evaluation of meteorite classification. In: Lauretta, D.S., McSween Jr., H.Y. (eds.) Meteorites and the Early Solar System II, pp. 19–52. The University of Arizona Press, Tucson, USA (2006)
2. Wasson J.T. Meteorites. Classification and Properties, Springer-Verlag: Berlin, Heidelberg, New York, 1974, pp. 1–320
3. Rubin, A.E., Ma, C.: Meteoritic minerals and their origins. Chem. Erde. **77**, 325–385 (2017)
4. Maksimova, A.A., Oshtrakh, M.I.: Applications of Mössbauer spectroscopy in meteoritical and planetary science, Part I: undifferentiated meteorites. Minerals. **11**, 612 (2021)
5. Maksimova, A.A., Goryunov, M.V., Oshtrakh, M.I.: Applications of Mössbauer spectroscopy in meteoritical and planetary science, part II: differentiated meteorites. Moon and Mars. Minerals. **11**, 614 (2021)
6. Mittlefehldt, D.W.: Asteroid (4) Vesta: I. The howardite-eucrite-diogenite (HED) clan of meteorites. Chem. Erde. **75**, 155–183 (2015)

7. Maksimova, A.A., Oshtrakh, M.I., Petrova, E.V., Grokhovsky, V.I., Semionkin, V.A.: Comparison of iron-bearing minerals in ordinary chondrites from H, L and LL groups using Mössbauer spectroscopy with a high velocity resolution. Spectrochim. Acta, Part A: Molec. and Biomolec. Spectroscopy. **172**, 65–76 (2017)
8. Kohout, T., Haloda, J., Halodová, P., Meier, M.M.M., Maden, C., Busemann, H., Laubenstein, M., Caffee, M.W., Welten, K.C., Hopp, J., Trieloff, M., Mahajan, R.R., Naik, S., Trigo-Rodriguez, J.M., Moyano-Cambero, C.E., Oshtrakh, M.I., Maksimova, A.A., Chukin, A.V., Semionkin, V.A., et al.: Annama H chondrite – mineralogy, physical properties, cosmic ray exposure, and parent body history. Meteorit. Planet. Sci. **52**, 1525–1541 (2017)
9. Maksimova, A.A., Oshtrakh, M.I., Chukin, A.V., Felner, I., Yakovlev, G.A., Semionkin, V.A.: Characterization of Northwest Africa 6286 and 7857 ordinary chondrites using X-ray diffraction, magnetization measurements and Mössbauer spectroscopy. Spectrochim. Acta, Part A: Molec. and Biomolec. Spectroscopy. **192**, 275–284 (2018)
10. Maksimova, A.A., Kamalov, R.V., Chukin, A.V., Felner, I., Oshtrakh, M.I.: An analysis of orthopyroxene from Tsarev L5 meteorite using X-ray diffraction, magnetization measurement and Mössbauer spectroscopy. J. Mol. Struct. **1174**, 6–11 (2018)
11. Oshtrakh, M.I., Maksimova, A.A., Goryunov, M.V., Petrova, E.V., Felner, I., Chukin, A.V., Grokhovsky, V.I.: Study of metallic Fe-Ni-Co alloy and stony part isolated from Seymchan meteorite using X-ray diffraction, magnetization measurement and Mössbauer spectroscopy. J. Mol. Struct. **1174**, 112–121 (2018)
12. Oshtrakh, M.I., Maksimova, A.A., Chukin, A.V., Petrova, E.V., Jenniskens, P., Kuzmann, E., Grokhovsky, V.I., Homonnay, Z., Semionkin, V.A.: Variability of Chelyabinsk meteoroid stones studied by Mössbauer spectroscopy and X-ray diffraction. Spectrochim. Acta, Part A: Molec. and Biomolec. Spectrosc. **219**, 206–224 (2019)
13. Maksimova, A.A., Petrova, E.V., Chukin, A.V., Karabanalov, M.S., Felner, I., Gritsevich, M., Oshtrakh, M.I.: Characterization of the matrix and fusion crust of the recent meteorite fall Ozerki L6. Meteorit. Planet. Sci. **55**, 231–244 (2020)
14. Maksimova, A.A., Unsalan, O., Chukin, A.V., Karabanalov, M.S., Jenniskens, P., Felner, I., Semionkin, V.A., Oshtrakh, M.I.: The interior and the fusion crust in Sariçiçek howardite: study using X-ray diffraction, magnetization measurements and Mössbauer spectroscopy. Spectrochim. Acta, Part A: Molec. and Biomolec. Spectrosc. **228**(2020), 117819
15. Maksimova, A.A., Petrova, E.V., Chukin, A.V., Karabanalov, M.S., Nogueira, B.A., Fausto, R., Yesiltas, M., Felner, I., Oshtrakh, M.I.: Characterization of Kemer L4 meteorite using Raman spectroscopy, X-ray diffraction, magnetization measurements and Mössbauer spectroscopy. Spectrochim. Acta, Part A: Molec. and Biomolec. Spectrosc. **242**, 118723 (2020)
16. Maksimova, A.A., Petrova, E.V., Chukin, A.V., Unsalan, O., Szabó, Á., Dankházi, Z., Felner, I., Zamyatin, D.A., Kuzmann, E., Homonnay, Z., Oshtrakh, M.I.: Study of Bursa L6 ordinary chondrite by X-ray diffraction, magnetization measurements and Mössbauer spectroscopy. Meteorit. Planet. Sci. **55**, 2780–2793 (2020)
17. Maksimova, A.A., Petrova, E.V., Chukin, A.V., Nogueira, B.A., Fausto, R., Szabó, Á., Dankházi, Z., Felner, I., Gritsevich, M., Kohout, T., Kuzmann, E., Homonnay, Z., Oshtrakh, M.I.: Bjurböle L/LL4 ordinary chondrite properties studied by Raman spectroscopy, X-ray diffraction, magnetization measurements and Mössbauer spectroscopy. Spectrochim. Acta, Part A: Molec. and Biomolec. Spectrosc. **248**, 119196 (2021)
18. Oshtrakh, M.I., Semionkin, V.A.: Mössbauer spectroscopy with a high velocity resolution: advances in biomedical, pharmaceutical, cosmochemical and nanotechnological research. Spectrochim. Acta, Part A: Molec. and Biomolec. Spectrosc. **100**, 78–87 (2013)
19. Oshtrakh M.I., Semionkin V.A. Mössbauer spectroscopy with a high velocity resolution: principles and applications. In Proceedings of the International Conference "Mössbauer Spectroscopy in Materials Science 2016", Tuček J., Miglierini M., Eds., AIP Conference Proceedings. AIP Publishing, Melville, New York, 2016, **1781**, 020019
20. Maksimova, A.A., Klencsár, Z., Oshtrakh, M.I., Petrova, E.V., Grokhovsky, V.I., Kuzmann, E., Homonnay, Z., Semionkin, V.A.: Mössbauer parameters of ordinary chondrites influenced by the fit accuracy of the troilite component: an example of Chelyabinsk LL5 meteorite. Hyperfine Interact. **237**, 33 (2016)
21. Maksimova A.A., Chukin A.V., Oshtrakh M.I. Revealing of the minor iron-bearing phases in the Mössbauer spectra of Chelyabinsk LL5 ordinary chondrite fragment. In Proceedings of the International Conference "Mössbauer Spectroscopy in Materials Science 2016", Eds. J. Tuček, M. Miglierini, AIP Conference Proceedings. AIP Publishing, Melville, New York, 2016, **1781**, 020016

22. Wang, H., Salveson, I.: A review on the mineral chemistry of the non-stoichiometric iron sulphide, $Fe_{1-x}S$ ($0 \leq x \leq 0.125$): polymorphs, phase relations and transitions, electronic and magnetic structures. Phase Transit. **78**, 547–567 (2005)
23. Maksimova, A.A., Petrova, E.V., Chukin, A.V., Oshtrakh, M.I.: Fe^{2+} partitioning between the M1 and M2 sites in silicate crystals in some stony and stony-iron meteorites studied using X-ray diffraction and Mössbauer spectroscopy. J. Mol. Struct. **1216**, 128391 (2020)
24. Rubin, A.E.: Kamacite and olivine in ordinary chondrites: intergroup and intragroup relationships. Geochim. Cosmochim. Acta. **54**, 1217–1232 (1990)
25. Kruse, O.: Mössbauer and X-ray study of the effects of vacancy concentration in synthetic hexagonal pyrrhotites. Am. Mineral. **75**, 755–763 (1990)
26. Vincze, I., Campbell, I.A., Meyer, A.J.: Hyperfine field and magnetic moments in b.c.c. Fe–Co and Fe–Ni. Solid State Commun. **15**, 1495–1499 (1974)
27. Valderruten, J.F., Alcazar, G.A.P., Greneche, J.M.: Study of Fe–Ni alloys produced by mechanical alloying. Phys. B Condens. Matter. **384**, 316–318 (2006)
28. Osborne, M.D., Fleet, M.E., Bancroft, G.M.: Fe^{2+}–Fe^{3+} ordering in chromite and Cr-bearing spinels. Contrib. Mineral. Petrol. **77**, 251–255 (1981)
29. Osborne, M.D., Fleet, M.E., Bancroft, G.M.: Next-nearest neighbor effects in the Mössbauer spectra of (Cr, Al) spinels. J. Solid State Chem. **53**, 174–183 (1984)
30. Lenaz, D., Skogby, H.: Structural changes in the $FeAl_2O_4$–$FeCr_2O_4$ solid solution series and their consequences on natural Cr-bearing spinels. Phys. Chem. Miner. **40**, 587–595 (2013)
31. Jastrzębska, I., Bodnar, W., Witte, K., Burkel, E., Stoch, P., Szczerba, J.: Structural properties of Mn-substituted hercynite. Nukleonika. **62**, 95–100 (2017)